# Accurate Relativistic Small-Core Pseudopotentials for Actinides. Energy Adjustment for Uranium and First Applications to Uranium Hydride[†]

**Michael Dolg* and Xiaoyan Cao**

*Institut für Theoretische Chemie, Universität zu Köln, Greinstrasse 4, D-50939 Köln, Germany*

*Received: May 13, 2009; Revised Manuscript Received: May 26, 2009*

The options to adjust accurate relativistic energy-consistent pseudopotentials for actinides are explored using uranium as an example. The choice of the reference data and the core−valence separation is discussed in view of a targeted accuracy of 0.04 eV or better in atomic energy differences such as excitation energies and ionization potentials. A new small-core pseudopotential attributing 60 electrons to the core has been generated by an energy adjustment to state-averaged multiconfiguration Dirac−Hartree−Fock/Dirac−Coulomb−Breit Fermi nucleus reference data of 100 nonrelativistic configurations of U to $U^{7+}$ corresponding to 30190 reference *J* levels. At the finite-difference multiconfiguration Hartree−Fock level the mean absolute errors are 0.002 and 0.024 eV for the configurations and J levels, respectively. A first molecular application to uranium monohydride UH yields very satisfactory agreement with results from all-electron calculations based on the Douglas−Kroll−Hess Hamiltonian.

## 1. Introduction

The effective core potential (ECP) approach, i.e., model potential (MP) and pseudopotential (PP) methods, are still the workhorse in relativistic quantum chemistry for heavy elements, despite the ongoing development of quite efficient approximate relativistic all-electron (AE) schemes.[1,2] Without doubt PPs lead to significant computational savings at the scalar-relativistic level, especially when inner shells of higher angular momenta, i.e., d or/and f shells, can be attributed to the PP core. At the correlated level the combination of PPs and effective core-polarization potentials (CPP) accounting for static and dynamic core polarization, i.e., polarization at the self-consistent field level and core−valence correlation, also leads to computational savings.

When spin−orbit (SO) interaction is included in two-step procedures, e.g., spin−orbit configuration interaction (SO-CI) starting from a scalar-relativistic Hartree−Fock (HF) reference[3,4] or even state interaction in the basis of highly correlated scalar-relativistic wave functions,[5,6] PPs allow the usage of effective valence SO operators, which implicitly include the relaxation of the occupied nonvalence orbitals under the SO term and thus limit the necessary size of the many-electron basis. Note that in order to achieve a sufficient relaxation of all shells under the influence of the SO operator, the corresponding AE approaches typically have to include single excitations from core orbitals in such two-step procedures or alternatively include the SO interaction already at the HF level, both strategies leading to an increased computational effort.[7]

In cases where contributions such as the Breit interaction are non-negligible, pseudopotentials also allow their inclusion in an implicit manner.[8] Thus, in principle they are able to go beyond the scope of standard AE schemes based solely on the full four-component Dirac−Coulomb (DC) Hamiltonian or two-component approximations of it, e.g., the Douglas−Kroll−Hess (DKH)[9−12] or Chang−Pelissier−Durand (CPD)[13] Hamiltonians.

As in all approximate computational schemes, PPs also have disadvantages. A basic limitation is the frozen-core approximation, although it is partly cured by effective CPPs. Accurate PPs which exhibit a high transferability between systems and a sound stability of the results with regard to extensions of the basis sets toward the basis set limit usually adopt a small-core model.[14] The additional nodal structure in the pseudovalence orbitals of small-core PPs compared to those of large-core PPs also improves the accuracy of valence correlation energies.

Among the most challenging systems for quantum chemical investigations and also for the PP adjustment are the actinides, especially those of the first half of the series which can adopt various oxidation states in their compounds.[15−18] The most interesting of these elements is probably uranium. As a heavy element (nuclear charge 92), it exhibits large relativistic effects, which increase roughly with the fourth power of the nuclear charge. Since the valence electrons are distributed in orbitals belonging to at least three different main and angular quantum numbers ($5f^3\ 6d^1\ 7s^2$ ground state configuration), with semicore closed shells ($6s^2\ 6p^6$) having a similar and core−shells ($5s^2\ 5p^6\ 5d^{10}$) having an only slightly smaller radial extension, large electron correlation effects are present, especially in energy differences between states where the occupation of the inner valence shells (5f, 6d) is changed.

In recent years accurate relativistic energy-consistent small-core PPs were generated for group 1,[19] group 2,[20] and groups 13−18 main group elements,[21−23] for groups 11 and 12[24] as well as first row,[25] second row,[26] and third row[27] transition metal elements. By means of construction these pseudopotentials model AE calculations based on the DC Hamiltonian, with a Fermi nuclear charge distribution and perturbatively including the Breit interaction (DC+B). All these potentials are accompanied by a series of correlation-consistent valence basis sets of the Dunning type, thus allowing for accurate extrapolations to the basis set limit.

In the present work we explore the construction of such PPs for uranium. One parametrization was selected and, together with an optimized valence basis set, was applied to study the molecular properties of the uranium hydride diatomic UH, which

[†] Part of the "Russell M. Pitzer Festschrift".

* Corresponding author: e-mail, m.dolg@uni-koeln.de; phone, +49-(0)221-4706893; fax, +49-(0)221-4706896 (M. Dolg).

10.1021/jp9044594 CCC: $40.75 
Published on Web 06/24/2009

was recently studied using an older Wood−Boring (WB) adjusted PP of the same core size.[28] The newly derived PP was already tested in SO-CI and intermediate Hamiltonian Fock-space coupled cluster (IH-FSCC) calculations[29,30] on $U^{5+}$ and $U^{4+}$, where it proved to be as accurate as AE calculations based on the DCB Hamiltonian.[31]

## 2. Method

The method of energy-consistent PPs and in particular their adjustment to MCDHF/DC+B total valence energies has been described in detail elsewhere,[21,25,14] and only a brief outline will be given. The 5f-in-valence PPs explored here treat 32 valence electrons in shells with main quantum number $n \geq 5$ explicitly, while those with $n < 5$ containing 60 electrons are attributed to the core. The following atomic valence-only model Hamiltonian was used.

$$\mathscr{H} = -\frac{1}{2}\sum_i \Delta_i + \sum_i V_{\mathrm{PP}}(\mathbf{r_i}) + \sum_{i<j}\frac{1}{r_{ij}} \qquad (1)$$

The kinetic energy term and core−electron and electron−electron interaction terms of $\mathscr{H}$ are nonrelativistic, all relativistic effects being implicitly included in the second term of $V_{\mathrm{PP}}$.

$$V_{\mathrm{PP}}(\mathbf{r}) = -\frac{Z_c}{r} + \sum_{ljk} B_{lj}{}^k \exp(-\beta_{lj}{}^k r^2)\mathscr{P}_{lj} \qquad (2)$$

The long-range behavior of $V_{\mathrm{PP}}$ is governed by the core charge $Z_c$, i.e., the first term of $V_{\mathrm{PP}}$, whereas the short-range part of $V_{\mathrm{PP}}$ is described by a semilocal ansatz, with the projection operators $\mathscr{P}_{lj}$ inducing different radial potentials for different angular-momentum quantum numbers $l$ and $j = l \pm 1/2$. The ansatz for the radial potentials, in turn, is a linear combination of Gaussians, and the parameters $B_{lj}{}^k$, $\beta_{lj}{}^k$ up to f symmetry were adjusted to four-component AE MCDHF/DC+B reference data,[32] which comprised 100 nonrelativistic configurations yielding a total of 30190 $J$ levels (cf. Supporting Information). The reference data were obtained for $U-U^{7+}$ and included a wide spectrum of occupations in the 5f, 6d, 7s, and 7p valence shells, but also additional configurations with holes in the core/semicore orbitals 5s, 5p, 5d, 6s, and 6p as well as configurations with electrons in the 6f−9f, 7d−9d, 8p−9p, and 8s−9s shells. Since the energetic position of the bare inner core relative to valence states is not expected to be notably relevant for chemical processes, the fit was restricted to the chemically more significant energy differences between valence states; i.e., a global shift was applied to all reference energies and treated as an additional parameter to be optimized[25]

$$\sum_I (\omega_I[E_I^{\mathrm{PP}} - E_I^{\mathrm{AE}} + \Delta E_{\mathrm{shift}}]^2) \doteqdot \min \qquad (3)$$

Here, $E_I^{\mathrm{PP}}$ and $E_I^{\mathrm{AE}}$ are the PP total valence energies and the AE valence energies (i.e., total energy minus energy of the bare core), respectively. The weights $\omega_I$ were chosen to be equal for all $J$ levels arising from a nonrelativistic configuration, and all nonrelativistic configurations were assigned to have equal weights. The global shift $\Delta E_{\mathrm{shift}}$ allows for the usage of configurations including core/semicore holes and can improve the accuracy of the fit by one or 2 orders of magnitude. For all U PPs mentioned here the global shift amounted to less than 1% of the ground state total valence energy.

We note that the PPs directly adjusted to MCDHF/DC+B reference data are designed to be used in two-component Hartree−Fock and subsequent electron correlation calculations or in two-component Kohn−Sham density functional studies. Results obtained within these schemes are directly comparable to corresponding ones from four-component AE calculations based on the Dirac Hamiltonian.

The molecular calculations were performed with the MOLPRO program system,[33] using both the newly adjusted U MCDHF/DC+B PP and the second-order DKH Hamiltonian.[9−11] At the AE and PP level newly optimized (30s26p18d14f7g)/[10s9p7d5f3g] and (14s13p10d8f6g)/[6s6p5d4f3g] ANO contracted basis sets were used for U (cf. Supporting Information), whereas for H the aug-cc-pVQZ basis set of Dunning was applied.[34] Scalar-relativistic calculations for the lowest ΛS states were performed at the complete active space self-consistent field (CASSCF) level followed by a multireference configuration interaction treatment including the Siegbahn size-extensivity correction (MRCI+Q). The need to restrict the active space to 5 electrons in 12 orbitals (in $C_{2v}$: 4 $a_1$, 3 $b_1$, 3 $b_2$, 2 $a_2$) was discussed in detail in the previous publication.[28] The U 5s, 5p, and 5d orbitals were kept frozen at the MRCI level. The Hamiltonian matrix including spin−orbit contributions was then built in the basis of the correlated ΛS states and diagonalized; i.e., the state interaction approach was applied. In the case of the AE treatment the spin−orbit contributions were evaluated for the Breit−Pauli (BP) Hamiltonian. In comparison to our previous work[28] three major improvements characterize the current calculations, i.e., the use of the better ANO basis sets also at the SO-CI level, the inclusion of a larger number of Λ S states in the SO−CI, and the application of the more accurate MCDHF/DC+B PP.

## 3. Results and Discussion

**3.1. Choice of the Reference Data.** A basic decision for the adjustment of a PP is the selection of the reference data, i.e., the relativistic computational model one aims to parametrize. The following discussion is restricted to multiconfiguration (MC) Dirac−Hartree−Fock/Dirac−Coulomb (DHF/DC) and Dirac−Coulomb−Breit (DHF/DC+B) as well as Wood−Boring (WB) all-electron (AE) reference data. In Table 1 results from relativistic AE DHF calculations[32] applying the DC Hamiltonian for the neutral and the 1-fold positively charged uranium atom are listed in the first data column (for a more extensive tabulation cf. the Supporting Information). The energy differences refer to averages over all $J$-levels (included in the MC treatment) of the listed nonrelativistic configurations. The DC Hamiltonian is a standard approximation used in four-component relativistic AE calculations for atoms, molecules, and solids. It captures the most important relativistic contributions which are relevant for quantum chemical studies of heavy element systems and thus has been used to generate reference data for the adjustment of, e.g., shape-consistent PPs.[35,36]

The importance of relativistic contributions for uranium can be seen in the second data column, which gives the deviations of nonrelativistic Hartree−Fock (HF) results from the MCDHF/DC reference data,[32] i.e., differential "nonrelativistic" contributions. The third data column lists deviations of scalar-relativistic one-component WB results from the MCDHF/DC reference data. The WB approach[37] and the related Cowan−Griffin (CG) approach[38] can be operated in the LS coupling scheme and were used to generate reference data for a large number of PPs, both

**TABLE 1: Relative Point Nucleus (pn) Dirac−Hartree−Fock/Dirac−Coulomb (DHF/DC) Energies $\Delta E$ (eV) of the $2J + 1$ Weighted Average of All $J$ Levels Belonging to a Nonrelativistic Configuration with Respect to the Energy of the U [Rn] $5f^3 6d^1 7s^2$ Ground State Configuration[a]**

| | configuration | | | | deviation | | contribution | |
|---|---|---|---|---|---|---|---|---|
| charge | 5f | 6d | 7s | $\Delta E$ DHF DC,pn | HF pn | WB pn | DHF DC,pn →B | DHF DC+B →fn |
| 1+ | | 4 | 1 | 16.0181 | 17.6511 | 0.7258 | 0.3111 | 0.0217 |
| 0 | | 4 | 2 | 9.7540 | 19.0413 | 0.7549 | 0.3200 | 0.0337 |
| 1+ | 1 | 3 | 1 | 9.6394 | 10.9340 | 0.4456 | 0.1929 | 0.0111 |
| 0 | 1 | 3 | 2 | 3.6701 | 12.1736 | 0.4714 | 0.2007 | 0.0218 |
| 1+ | 2 | 1 | 2 | 5.7548 | 7.8467 | 0.2722 | 0.1031 | 0.0194 |
| 0 | 2 | 2 | 2 | 0.4682 | 5.8033 | 0.2236 | 0.0933 | 0.0105 |
| 1+ | 3 | | 2 | 4.4832 | 1.9041 | 0.0435 | 0.0073 | 0.0084 |
| 0 | 3 | 1 | 2 | 0.0000 | 0.0000 | 0.0000 | 0.0000 | 0.0000 |
| 1+ | 4 | | 1 | 6.8681 | −5.8095 | −0.1977 | −0.0817 | −0.0156 |
| 0 | 4 | | 2 | 2.0435 | −5.1113 | −0.1784 | −0.0749 | −0.0094 |
| 1+ | 5 | | | 12.5023 | −11.2231 | −0.3303 | −0.1358 | −0.0313 |
| 0 | 5 | | 1 | 8.1022 | −10.2666 | −0.2698 | −0.1171 | −0.0231 |

[a] For each 5f occupation number only the energetically lowest configuration for each ionization level is listed. Deviations (eV) from the DHF/DC pn data are given for nonrelativistic Hartree−Fock (HF) and scalar-relativistic Wood−Boring (WB) pn calculations. Contributions of the Breit interaction (→B) at the DHF/DC pn level as well as of a finite nucleus (→fn) with a Fermi charge distribution at the DHF/DC+B level are also listed.

**TABLE 2: As Table 1, but for All-Electron Point Nucleus (pn) Wood−Boring and Finite Fermi Nucleus (fn) Dirac−Hartree−Fock/Dirac−Coulomb−Breit (DHF/DC+B) Energy Differences $\Delta E$ (eV) with Respect to the Uranium Ground State[a]**

| | configuration | | | | | | $\Delta\Delta E$ | |
|---|---|---|---|---|---|---|---|---|
| charge | 5f | 6d | 7s | $\Delta E$ WB pn | $\Delta\Delta E$ SPP old | $\Delta E$ DHF DC+B,fn | SPP new | GRECP |
| 1+ | | 4 | 1 | 16.7440 | −0.0173 | 16.3620 | −0.0045 | |
| 0 | | 4 | 2 | 10.5089 | 0.0404 | 10.1180 | −0.0038 | |
| 1+ | 1 | 3 | 1 | 10.0850 | −0.0093 | 9.8506 | 0.0009 | 0.0843 |
| 0 | 1 | 3 | 2 | 4.1415 | 0.0344 | 3.8992 | 0.0012 | 0.0843 |
| 1+ | 2 | 1 | 2 | 6.0270 | 0.0453 | 5.8808 | 0.0012 | 0.0467 |
| 0 | 2 | 2 | 2 | 0.6918 | 0.0095 | 0.5751 | 0.0014 | 0.0449 |
| 1+ | 3 | | 2 | 4.5267 | 0.0273 | 4.4993 | −0.0017 | 0.0011 |
| 0 | 3 | 1 | 2 | 0.0000 | 0.0000 | 0.0000 | 0.0000 | 0.0000 |
| 1+ | 4 | | 1 | 6.6705 | 0.0010 | 6.7689 | −0.0011 | −0.0454 |
| 0 | 4 | | 2 | 1.8651 | 0.0129 | 1.9568 | 0.0005 | −0.0450 |
| 1+ | 5 | | | 12.1721 | 0.0459 | 12.3320 | 0.0034 | −0.0832 |
| 0 | 5 | | 1 | 7.8323 | 0.0617 | 7.9585 | 0.0043 | |

[a] The errors $\Delta\Delta E$ (eV) are listed for a Wood−Boring (WB) adjusted (old)[53] as well as a Dirac−Hartree−Fock/Dirac−Coulomb−Breit adjusted (this work) small-core pseudopotential (SPP). For comparison available data from literature for a generalized relativistic effective core potential (GRECP) adjusted to fn DHF/DCB data are also listed.[45]

shape-consistent[39−41] and energy-consisten,t[42,43] as well as MPs.[44] The data listed in Table 1 reveals that although the WB approach captures to a large extent the relativistic contributions, it also introduces some inaccuracies especially when the 5f occupation is changed. The WB and CG schemes are therefore not suitable to generate reference data for PPs when high accuracy is desired.

The contributions of the Breit interaction, in its frequency-dependent form as implemented in the GRASP[32] atomic structure package, evaluated in first-order perturbation based on a MCDHF solution obtained with the DC Hamiltonian (denoted as DC+B) are listed in the fourth data column. These contributions are weakly dependent on the 5f occupancy and can amount to a few tenths of an electronvolt. For the 30190 $J$ levels considered in the PP adjustment the root mean squared deviation (rmsd) between DC and DC+B valence energies is 0.109 eV, when a global shift is applied to all levels of one sequence in order to obtain the best possible agreement. The low-frequency limit DC+B valence energies show a RSMD of only 0.004 eV to the frequency-dependent values. The self-consistent treatment of the Breit term (denoted as DCB) contributes to relative energies of U and $U^+$ as listed in Table 1 with at most 0.0005 eV;[45] i.e., in view of a targeted accuracy of 0.04 eV in atomic energy differences a perturbative treatment (denoted as DC+B) is accurate enough to generate reliable AE reference data for PP adjustments.

In the fifth data column the contributions of a finite nuclear model, i.e., a Fermi nuclear charge distribution, are listed. These contributions turn out to be quite small, and the applied nuclear model is probably of little importance for studies of the valence electronic structure. Although the latter are the goal of PP calculations, finite nucleus effects can be included implicitly in the PP adjustment without additional computational effort. The more recent so-called "Stuttgart" energy-consistent relativistic PPs are based on reference energies obtained at the AE MCDHF/DC+B level applying a Fermi finite nuclear model.[19−27] In the case of the 30190 $J$ levels considered here, the point nucleus DC+B valence energies show a rmsd of 0.017 eV from the corresponding Fermi finite nucleus values, again after a global shift applied to all levels of one sequence in order to obtain the best possible agreement.

**TABLE 3: Relative Energies (eV) of the $(2J + 1)$-Weighted Average of All $J$ Levels Belonging to a Nonrelativistic Configuration of U with Respect to the U [Rn] $5f^3 6d^1 7s^2$ Ground State Configuration from All-Electron (AE) Point Nucleus (pn) State-Averaged Multiconfiguration Dirac−Hartree−Fock (DHF) Calculations Using the Dirac−Coulomb (DC) Hamiltonian[32a]**

| | configuration | | | AE DHF | frozen-core error | | |
|---|---|---|---|---|---|---|---|
| charge | 5f | 6d | 7s | DC,pn | $Q = 32$ | $Q = 14$ | $Q = 6$ |
| 1+ | | 4 | 1 | 16.0181 | 0.0039 | 0.7379 | 3.8610 |
| 0 | | 4 | 2 | 9.7540 | 0.0038 | 0.7365 | 3.5686 |
| 1+ | 1 | 3 | 1 | 9.6394 | 0.0013 | 0.3082 | 1.6778 |
| 0 | 1 | 3 | 2 | 3.6701 | 0.0013 | 0.3046 | 1.5126 |
| 1+ | 2 | 1 | 2 | 5.7548 | 0.0001 | 0.0636 | 0.5841 |
| 0 | 2 | 2 | 2 | 0.4682 | 0.0002 | 0.0678 | 0.3493 |
| 1+ | 3 | | 2 | 4.4832 | 0.0000 | 0.0009 | 0.0412 |
| 0 | 3 | 1 | 2 | 0.0000 | 0.0000 | 0.0000 | 0.0000 |
| 1+ | 4 | | 1 | 6.8681 | 0.0001 | 0.0450 | 0.2224 |
| 0 | 4 | | 2 | 2.0435 | 0.0002 | 0.0426 | 0.2430 |
| 1+ | 5 | | | 12.5023 | 0.0004 | 0.0945 | 0.6651 |
| 0 | 5 | | 1 | 8.1022 | 0.0004 | 0.0761 | 0.5418 |

[a] Frozen-core errors (eV) are listed for three choices of the core (core charges $Q = 32$, 14, 6) treating the 5f shell in the valence adapted from the neutral U atom in its [Rn] $5f^3 6d^1 7s^2$ ground state configuration. Frozen cores: U $Q = 6$, 1s−5d, 6s, 6p; $Q = 14$, 1s−5d; $Q = 32$, 1s−4d.

Other contributions, e.g., those arising from quantum electrodynamics such as vacuum polarization and electron self-energy, are typically smaller than those of the nuclear model and thus can be safely neglected when constructing a valence model Hamiltonian aiming at chemical accuracy, i.e., 1 kcal/mol (0.04 eV).

**3.2. Choice of the Core.** In the case of uranium, one essentially has three possibilities for the choice of the core: small, medium, and large. Relativistic AE atomic frozen-core (FC) calculations can be used as guidance to which errors might result from freezing cores of different sizes. Table 3 lists frozen core results for the same configurations as included in Table 1 (for a more extensive tabulation cf. the Supporting Information). The frozen core was taken from a state-averaged MCDHF/DC calculation for the U [Rn] $5f^3 6d^1 7s^2$ ground state configuration. In order to achieve significant computational savings, a core as large as possible is desired. However, the data listed in Table 3 reveal that treating U with only six valence electrons ($Q = 6$), i.e., assuming a large core (1s−5d, 6s, 6p) in line with qualitative chemical models, quantitatively leads to FC errors of up to several electronvolts when the 5f occupation is changed. In comparison to this a medium-sized core (1s−5d), attributing the 6s and 6p semicore orbitals to the valence shell, which now comprises 14 valence electrons ($Q = 14$), yields FC errors of at most about 1 eV, whereas a small core (1s−4f) treating 32 electrons in the valence ($Q = 32$) leads to errors of less than 0.01 eV.

The conclusions reached with regard to the FC errors for the few configurations listed in Table 3 remain valid when looking at an extended set of over 60 configurations (18, 15, 12, 9, 6, and 3 with $5f^0$, $5f^1$, $5f^2$, $5f^3$, $5f^4$, and $5f^5$, respectively), which contains for each 5f occupation several different 6d occupations. For a fixed 5f occupation a small dependency of the FC errors on the 6d occupation is observed. This is noticeable for the medium-core and especially the large-core cases, but the effects are less pronounced than the dependency on the 5f occupation. We note here in passing that these results allow us to adjust the so-called 5f-in-core PPs, i.e., PPs which adopt a medium-core definition and in addition attribute the open 5f shell to the PP core, thus modeling an actinide element with a fixed valency.[46−48] These PPs allow quantum chemical calculations to be performed on superconfigurations[49] of actinide systems with relatively low computational effort. Care has to be taken not to go beyond the range of applicability of these PPs; however, for systems where the 5f shell remains corelike and does not participate significantly in chemical bonding, the results are very encouraging.[50−52]

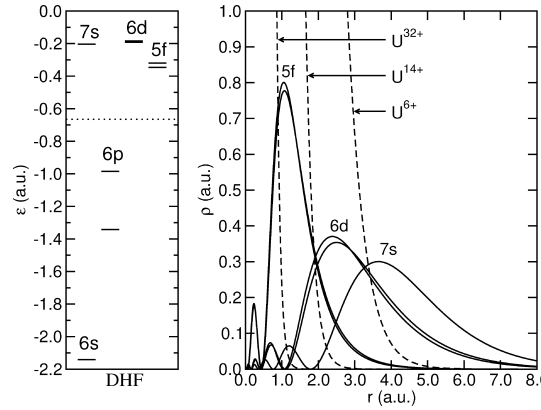


**Figure 1.** One-particle energies and corresponding radial densities for the 5f, 6d, and 7s spinors of uranium in its [Rn] $5f^3 6d^1 7s^2$ ground state configuration as well as corresponding $U^{6+}$, $U^{14+}$, and $U^{32+}$ core densities from all-electron Dirac−Hartree−Fock/Dirac−Coulomb calculations.

The origin of the FC errors can be made plausible from a graphical representation of the uranium orbital energies, the corresponding radial orbital densities, and the core densities (Figure 1). From an energy point of view, e.g., looking at the orbital energies, the 5f, 6d, and 7s shells belong to the valence space, whereas the 6p, 6s, and all other shells at lower one-particle energies belong to the core space. However, from a spatial point of view, e.g., looking at the radial densities, one observes that the 5f shell is more compact than the core densities of a large-core ($U^{6+}$) and medium-core ($U^{14+}$) definition. Thus a change in the 5f occupation number changes the effective nuclear charge experienced by the 6s and 6p semicore shells and leads to large FC errors when these are put into the core. Smaller, but for high accuracy non-negligible FC errors arise when the 5s, 5p, and 5d shells are put into the core since these have a similar radial extension as the 5f shell, as can be seen from a comparison of the small-core ($U^{32+}$) and medium-core ($U^{14+}$) densities. The same is true for the 6s and 6p semicore shells with respect to the 6d valence shell. Thus, from a spatial point of view it is clear that for accurate calculations all orbitals with main quantum number $n \geq 5$ have to be treated in the valence space. The currently available small-core PPs for the actinides use this core definition,[53,54] which corresponds to the one adopted for small-core lanthanide PPs[55,56] where all shells with main quantum number $n \geq 4$ are treated in the valence space.

It still might be possible to reduce the number of valence electrons from 32 to 30 or 24 by including the 5s or 5s and 5p shells to the core. However, the computational savings are relatively small since only low angular momenta basis functions can be saved. Moreover, in correlated calculations using pseudovalence orbitals, errors due to the eliminated radial nodes may arise. No detailed investigation of these effects exists for the uranium atom; however studies of main group elements[57−60] point to a possible overestimation of exchange integrals between, e.g., the (5f, 6d) and (7s, 7p) shells and thus a possible

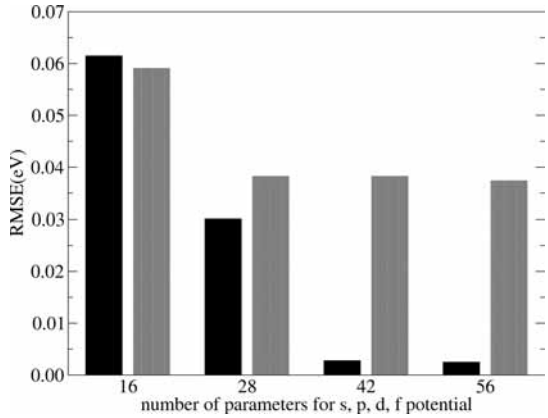


**Figure 2.** RMSE (eV) for the configurational average (black) and the individual *J* levels (gray) of Dirac-Hartree−Fock/Dirac−Coulomb−Breit Fermi nucleus adjusted small-core pseudopotentials for uranium with different number of parameters. The entries 16, 28, 42, and 56 on the abscissa correspond roughly to one, two, three, and four Gaussian terms per *lj* value in the radial expansion of the s, p, d, and f pseudopotentials (cf. text). The reference data sets comprised 100 nonrelativistic configurations and the associated 30190 *J* levels.

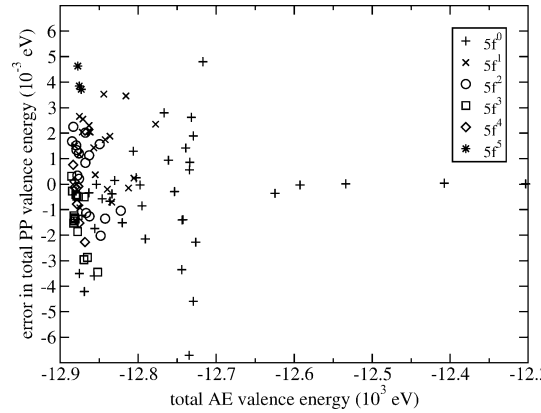


**Figure 3.** Errors (eV) in total valence energies of 100 nonrelativistic configurations for the multiconfiguration Dirac−Hartree−Fock/Dirac−Coulomb−Breit Fermi nucleus adjusted small-core pseudopotential for uranium. RMSE = 16.1 $cm^{-1}$, MAE = 12.3 $cm^{-1}$.

overestimation of related correlation contributions as well as multiplet splittings.

**3.3. Pseudopotential Adjustment.** The uranium PP presented here is directly adjusted to MCDHF reference data obtained for the DCB Hamiltonian with a Fermi nuclear charge distribution.[32] The two-component MCHF PP calculations were performed in the same (intermediate) coupling scheme. Since both AE and PP calculations were carried out at the finite difference level, errors due to the use of finite basis sets were avoided. The reference data set used to determine the PP up to f symmetry comprised 100 nonrelativistic configurations yielding a total of 30190 *J* levels. It was obtained for $U-U^{7+}$ and included a wide spectrum of occupations in the 5f, 6d, 7s, and 7p valence shell (occupation numbers 5f, 0−5; 6d, 0−4; 7s, 0−2; 7p, 0−1) but also additional configurations with holes in the core/semicore shells 5s, 5p, 5d, 6s, 6p as well as configurations with electrons in the 6f−9f, 7d−9d, 8p−9p, and 8s−9s shells. The complete list of reference configurations is provided in the auxiliary material. The g-part of the PP was adjusted to the eight energetically lowest $U^{31+}$ [Kr] $4d^{10}4f^{14}ng^1$ ($n = 5-12$) configurations, a fit which is virtually exact.

Since due to the SO splitting of the shells with angular quantum number $l > 0$, $V_l$ is divided into two components, $V_{l,j=l-1/2}$ and $V_{l,j=l+1/2}$, and the number of parameters for a PP up to f symmetry with *m* Gaussians per *lj* term is thus 14*m*. Test calculations using DHF/DC+B(frequency-dependent) Fermi nucleus reference data revealed that for the reference states included in the adjustment at least two Gaussians have to be used in s symmetry in order to get a satisfactory accuracy; i.e., the minimum number of adjustable parameters was 16. Figure 2 shows the development of the root mean squared error (RMSE) of the energies of the nonrelativistic configurations as well as of the individual *J* levels when the number of adjustable parameters increases. Whereas the error with respect to the individual *J* levels seems to be converged already with two Gaussians per *lj* term to about 300 $cm^{-1}$ (0.037 eV), the one for the averages of the configurations can be further reduced to below 20 $cm^{-1}$ (0.002 eV) by applying four Gaussians per *lj* value.

Figure 3 gives an overview of the errors for the configurational averages for the most extensive parametrization with four Gaussians per *lj* term (56 parameters) in the case of MCDHF/DC+B(low frequency limit) Fermi nucleus reference data. In contrast to the AE FC errors listed in Table 3 the PP errors exhibit a less systematic behavior with respect to the 5f occupancy; however, their magnitude is comparable and stays below 0.012 eV for any energy difference between two of the configurations in a total energy interval of approximately 600 eV. The RMSE of the valence energies is 0.0020 eV (16.1 $cm^{-1}$), their MAE is 0.0015 eV (12.3 $cm^{-1}$).

Table 2 summarizes PP errors with respect to relative AE energies. It should be noted that the configurations listed there form a small subset of the reference configurations used in the PP adjustment. For comparison results published for a shape-consistent (generalized) relativistic effective core potential (GRECP) are also listed.[45] This PP was also adjusted to DHF/DCB reference data, however not at the MC level. It combines the traditional semilocal with a nonlocal ansatz. PPs of this school exhibit a fairly high accuracy, but the number of adjustable parameters is significantly larger than those for the energy-consistent case and the additional nonlocal term cannot be handled by most quantum chemistry codes, including the ones accessible to us. Thus our conclusions are only based on the data available from the original publication. It can be seen that a characteristic pattern of errors, i.e., a clear dependency on the f occupancy *n* with roughly $(3 - n)0.043$ eV, results.

The behavior of the errors for the individual *J* levels is displayed in Figure 4 for the MCDHF/DC+B-adjusted PP. The RMSE is 0.038 eV (305.8 $cm^{-1}$) and the MAE is 0.024 eV (196.5 $cm^{-1}$). The largest error is 0.267 eV and occurs for a very high-lying *J* level of a chemically probably not too important configuration with a $5f^4$ occupation. If only *J* levels with a relative energy of 5 eV with respect to the lowest *J* level of the configuration are considered, the maximum error is below 0.1 eV, and if only the lowest *J* levels of each configuration are considered, it is at most 0.036 eV. Again we compare to the GRECP, restricting ourselves to two data sets out of three taken from the original publication.[45] It can be seen from Table 4 that for the individual *J* levels, when described as a single determinant in the *jj* coupling scheme, the errors of the energy-consistent PP are slightly smaller than the ones obtained for the GRECP. The same is true for the third data set not shown here.

Since only energy information and no orbital information enters the PP fit, it is interesting to see how well the AE valence orbitals are approximated by the PP pseudovalence orbitals in the spatial valence region. Figure 5 shows such a comparison

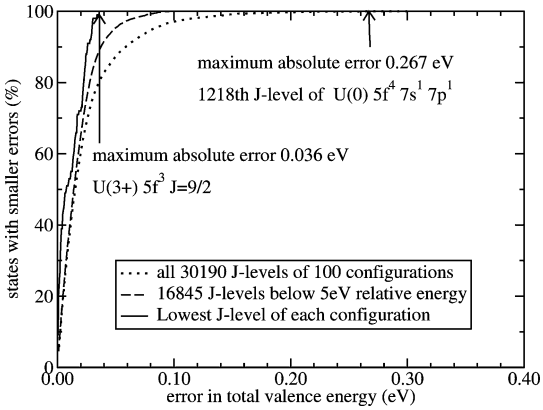


**Figure 4.** Percentage (%) of $J$ levels with errors in the total valence energies below the threshold (eV) indicated on the abscissa for the multiconfiguration Dirac−Hartree−Fock/Dirac−Coulomb−Breit Fermi nucleus adjusted small-core pseudopotential for uranium. RMSE = 305.8 $cm^{-1}$, MAE = 196.5 $cm^{-1}$.

for the U ground state. It is obvious that the agreement between MCDHF/DC+B PP and AE DHF/DC spinors in the spatial valence region is excellent. In this context we want to note that in the shape-consistent formalism an exact agreement between pseudovalence orbitals and all-electron orbitals in the spatial valence region is only required for a single reference state.

**3.4. Basis Set Optimization.** A (14s13p10d8f6g)/[6s6p5d4f3g] basis set has been generated for the new MCDHF/DC+B PP essentially following the procedure used for the generation of the basis sets for the older actinide WB PPs.[54] First a (14s11p8d8f) set of exponents was energy-optimized in atomic PP HF calculations using Pitzer's ATMSCF code[61] for the [Rn] $5f^4 7s^2$ $^5$I state of the neutral uranium atom. In the second step two diffuse d functions for the description of the 6d shell were HF energy-optimized for the [Rn] $5f^3 6d^1 7s^2$ $^5$L state. In order to describe the 7p shell, two diffuse p functions were optimized for the [Rn] $5f^3 7s^2 7p^1$ $^5$I state in the third step. In order to guarantee an unbiased description of states with different 5f occupation, the contraction coefficients for the resulting (14s13p10d8f)/[6s6p5d4f] sets were obtained in the fourth step from averaged density matrices for the lowest LS states of the [Rn] $5f^3 6d^1 7s^2$ and [Rn] $5f^4 7s^2$ configurations. Symmetry-breaking at the CASSCF level was avoided by averaging over all components of each LS state. Whereas it was feasible to perform CASSCF/MRCI calculations for the [Rn] $5f^4 7s^2$ $^5$I state, the [Rn] $5f^3 6d^1 7s^2$ $^5$L state only could be treated at the CASSCF level. In the MRCI calculations the 5s, 5p, and 5d shells were kept frozen; i.e., the basis set is suitable for correlating the 5f and $n > 5$ shells, whereas additional functions should be added when a correlation of the 5s, 5p, and 5d shells is also desired. Finally, as the fifth and last step, six g exponents were chosen identically to the six largest f exponents. This choice reflects their importance in the g ANOs obtained from MRCI calculations for the [Rn] $5f^4 7s^2$ $^5$I state using the (14s13p10d8f)/[6s6p5d4f] ANO basis set augmented by eight g exponents identical to those of the f set. A generalized ANO contraction was derived as described above for the [Rn] $5f^4 7s^2$ $^5$I state, yielding the final (14s13p10d8f6g)/[6s6p5d4f3g] set. Since 5s, 6s, 5p, 6p, and 5d have to be attributed to the semicore orbitals and are described with one contraction each, a [4s4p4d4f3g] set is left for the description of the 5f, 6d, 7s, and 7p valence shells; i.e., a set of overall polarized valence quadruple-$\zeta$ quality arises. Sets of polarized triple- and double-$\zeta$ quality as well as a minimal basis set can be easily created by omitting contractions with small ANO occupation numbers. The basis set errors in the total valence energies at the HF level amount to less than 0.003 Hartrees for all these basis sets.

**3.5. Uranium Monohydride.** In a recent study we compared results for uranium monohydride UH[28] obtained with a WB-adjusted relativistic U small-core PP[53] and AE data derived with the scalar-relativistic Douglas−Kroll−Hess Hamiltonian (DKH)[9−11] augmented by the Breit−Pauli (BP) SO Hamiltonian. Although a very good agreement between the AE and PP results was observed (e.g., $\Omega = 9/2$ ground state: DKH $R_e$ =2.021 Å, $\omega_e$ =1483 $cm^{-1}$, $D_e$ =2.79 eV; PP $R_e$ =2.011 Å, $\omega_e$ =1497 $cm^{-1}$, $D_e$ =2.85 eV), some deficiencies remained in both calculations. At the AE level only a very small uncontracted basis set could be used to evaluate the SO contributions, whereas at the PP level the SO term associated to the WB-adjusted PP is not highly accurate. Moreover only the lowest $\Lambda$S states were included into the SO-CI. In the present these deficiencies are all removed, i.e., the same U AE spdf ANO basis set as used for the scalar-relativistic calculations was applied in the SO-CI, the WB PP was replaced by the more acccurate MCDHF/DC+B PP, and more low-lying excited states (cf. below) were included in the SO-CI.

The electronic structure of UH was previously discussed in more detail[28] and only a brief overview will be given. Assuming an ionic compound $U^+$ $H^-$, one can expect that the lowest electronic states arise from the $U^+$ $5f^3$ $7s^2$ $^4$I ground state as well as the $U^+$ $5f^3$ $6d^1$ $7s^1$ $^6$L state, for which the lowest $^6L_{11/2}$ level experimentally is found to be only 289 $cm^{-1}$ above the $^4I_{9/2}$ ground level. Thus $^4\Lambda$ ($\Lambda = 0-6$) and $^6\Lambda$ ($\Lambda = 0-8$) molecular states with an approximately atomic-like $5f^3$ subconfiguration on U are expected to be lowest in energy.

Table 5 summarizes our CASSCF/MRCI+Q results for these states. The mean absolute deviation (MAD) between the PP and AE results is for the quartet and sextet states, respectively, 0.005 and 0.003 Å in $R_e$, 23.6 $cm^{-1}$ and 56.6 $cm^{-1}$ in $\omega_e$, and 0.003 and 0.066 eV in $T_e$. If term energies with respect to the lowest sextet state, the last number reduces to 0.002 eV. When replacing the second-order by a third-order DKH Hamiltonian at the CASSCF level, the term energies of the sextet states are increased by about 0.014 eV and the agreement between PP and AE results is slightly improved. The term energies of the quartet states change by less than 0.001 eV, and bond lengths and vibrational frequencies of both quartet and sextet states change by at most 0.001 Å and 1 $cm^{-1}$, respectively.

For the $^4$I ground state we obtained 2.021 and 2.017 Å for $R_e$, 1499 and 1522 $cm^{-1}$ for $\omega_e$, and 3.04 and 2.99 eV for $D_e$ at the PP and AE CASSCF/MRCI+Q level, respectively. The slightly better agreement obtained previously[28] was partly fortuitous; i.e., it is partly due to the selection of reference configurations for the MRCI, which had to be performed in the older work in the AE case in order to keep the problem tractable. Upon inclusion of SO coupling the results are 2.025 and 2.021 Å for $R_e$, 1505 and 1511 $cm^{-1}$ for $\omega_e$, and 2.82 and 2.79 eV for $D_e$. The results obtained with the new MCDHF/DC+B PP are in somewhat better agreement with the AE DKH results than was the case for the old WB PP; however, a perfect agreement cannot be expected. Whereas both the second-order DKH approach and the WB approach underlying the old PP aim to model results obtained with a spin-free DC Hamiltonian, the new PP is adjusted to MCDHF/DC+B data which include additional effects. In addition, a construction of finite AE and PP basis sets without any bias is almost impossible.

The only experimental data available so far is an infrared absorption at 1424 $cm^{-1}$, observed for the major products of the reaction of laser-ablated uranium atoms with $H_2$ in an Ar matrix, which is assigned to UH.[62] This value deviates quite

**TABLE 4: Relative Energies $\Delta E$ ($cm^{-1}$) for Single-Determinant $J$ Levels Calculated at the Dirac−Hartree−Fock/Dirac−Coulomb−Breit (DHF/DC+B,DCB) Level Using a Fermi Charge Distribution for the Finite Nucleus and Errors $\Delta\Delta E$ ($cm^{-1}$) of Calculations with a Small-Core Energy-Consistent Pseudopotential (SPP) (this work) and a Generalized Relativistic Effective Core Potential (GRECP)[45] Modeling Such All-Electron Calculations[a]**

| | $5f_-{}^3 6d_-{}^1 7s_+{}^2$ | | | | $5f_-{}^2 6d_-{}^2 7s_+{}^2$ | | | |
|---|---|---|---|---|---|---|---|---|
| $J$ | $\Delta E$ DHF DC+B | $\Delta\Delta E$ SPP | $\Delta E$ DHFDCB | $\Delta\Delta E$ GRECP | $\Delta E$ DHF DC+B | $\Delta\Delta E$ SPP | $\Delta E$ DHF DCB | $\Delta\Delta E$ GRECP |
| 0 | 10767.4 | 366.0 | 10767 | 416 | 39561.1 | 422.6 | 39562 | 724 |
| 1 | 29342.5 | 311.6 | 29343 | 553 | 20452.5 | 101.2 | 20453 | 292 |
| 2 | 20477.0 | 413.4 | 20477 | 556 | 24250.8 | 228.8 | 24252 | 422 |
| 3 | 18515.7 | 208.6 | 18516 | 359 | 15905.0 | −38.9 | 15906 | 126 |
| 4 | 17458.4 | 194.0 | 17458 | 339 | 13548.7 | −20.7 | 13549 | 86 |
| 5 | 2762.4 | −55.4 | 2762 | −23 | 7017.3 | −116.5 | 7018 | −30 |
| 6 | 0.0 | 0.0 | 0 | 0 | 0.0 | 0.0 | 0 | 0 |
| MAE | | 258.2 | | 374.3 | | 154.8 | | 280.0 |

[a] Mean absolute errors ($cm^{-1}$) are listed in the last line.

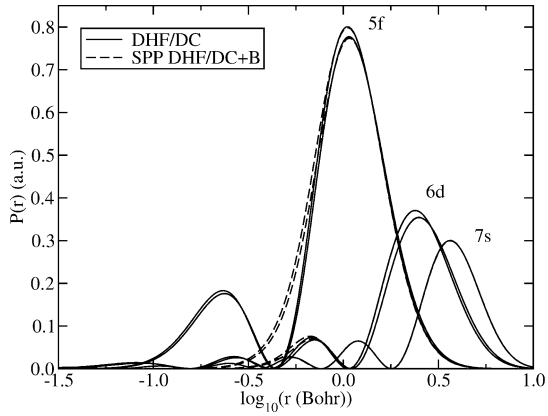


**Figure 5.** Radial one-particle densities of 5f, 6d, and 7s of uranium in the [Rn] $5f^3 6d^1 7s^2$ ground state configuration from state-averaged multiconfiguration Dirac−Hartree−Fock/Dirac−Coulomb calculations[32] in comparison to pseudovalence one-particle densities obtained from calculations with the two-component Dirac−Hartree−Fock/Dirac−Coulomb−Breit adjusted small-core pseudopotential presented in this work.

**TABLE 5: Bond Lengths $R_e$ (Å), Vibrational Constants $\omega_e$ ($cm^{-1}$), and Adiabatic Term Energies $T_e$ (eV) of UH from AE DKH and MCDHF/DC+B PP MRCI+Q Calculations without Spin−Orbit Coupling[a]**

| | $R_e$ | | $\omega_e$ | | $T_e$ | |
|---|---|---|---|---|---|---|
| state | PP | AE | PP | AE | PP | AE |
| $^4\Gamma$ | 2.021 | 2.017 | 1499 | 1522 | 0.000 | 0.000 |
| $^4\Phi$ | 2.025 | 2.019 | 1495 | 1518 | 0.028 | 0.022 |
| $^4\Gamma$ | 2.022 | 2.017 | 1490 | 1514 | 0.046 | 0.046 |
| $^4\Phi$ | 2.020 | 2.015 | 1488 | 1515 | 0.061 | 0.058 |
| $^4\Delta$ | 2.021 | 2.016 | 1486 | 1511 | 0.063 | 0.063 |
| $^4\Pi$ | 2.024 | 2.018 | 1487 | 1509 | 0.077 | 0.073 |
| $^4\Sigma$ | 2.026 | 2.020 | 1486 | 1507 | 0.099 | 0.092 |
| $^6\Lambda$ | 2.067 | 2.066 | 1440 | 1382 | 0.430 | 0.363 |
| $^6$K | 2.066 | 2.063 | 1439 | 1380 | 0.446 | 0.378 |
| $^6$I | 2.064 | 2.061 | 1432 | 1374 | 0.486 | 0.420 |
| $^6$H | 2.063 | 2.060 | 1432 | 1378 | 0.522 | 0.457 |
| $^6\Gamma$ | 2.063 | 2.061 | 1427 | 1367 | 0.546 | 0.482 |
| $^6\Phi$ | 2.063 | 2.060 | 1428 | 1366 | 0.584 | 0.521 |

[a] Key: PP, MCDHF/DC+B PP; AE, DKH.

significantly from our current and previous results for $\omega_e$ (1483 (PP) and 1497 (AE) $cm^{-1}$),[28] as it does for recent PP/SO-CI results published by Balasubramanian and co-workers (1538 $cm^{-1}$)[63] and scalar-relativistic AE DFT results of Andrews and co-workers (1480 $cm^{-1}$).[64] However, after estimating the anharmonicity from a Morse potential, one obtains frequencies of 1455 and 1460 $cm^{-1}$ at the CASSCF/MRCI+SO level for the present PP and AE calculations. The remaining deviation of about 30−35 $cm^{-1}$ might in part be due to matrix effects.

**TABLE 6: Vertical Term Energies (eV) of UH at 2.011 Å from Calculations with Spin-Orbit Coupling (State Interaction Approach)[f]**

| | | SPP | | | AE DKH | | |
|---|---|---|---|---|---|---|---|
| no. | Ω | WB[a,b,d] | DC+B[b,e] | DC+B[c,e] | +BP[a,b,d] | +BP[b,e] | +BP[c,e] |
| 1 | 4.5 | 0.000 | 0.000 | 0.000 | 0.000 | 0.000 | 0.000 |
| 2 | 3.5 | 0.032 | 0.029 | 0.026 | 0.039 | 0.032 | 0.020 |
| 3 | 2.5 | 0.046 | 0.046 | 0.043 | 0.056 | 0.049 | 0.038 |
| 4 | 1.5 | 0.057 | 0.058 | 0.055 | 0.066 | 0.060 | 0.053 |
| 5 | 0.5 | 0.068 | 0.070 | 0.067 | 0.077 | 0.071 | 0.066 |
| 8 | 5.5 | 0.336 | 0.380 | 0.374 | 0.419 | 0.419 | 0.410 |
| 10 | 4.5 | 0.363 | 0.405 | 0.401 | 0.455 | 0.447 | 0.432 |
| 11 | 3.5 | 0.378 | 0.424 | 0.419 | 0.469 | 0.464 | 0.454 |
| 12 | 2.5 | 0.392 | 0.436 | 0.431 | 0.484 | 0.480 | 0.478 |
| 13 | 1.5 | 0.402 | 0.454 | 0.448 | 0.494 | 0.491 | 0.478 |
| 14 | 0.5 | 0.404 | 0.452 | 0.448 | 0.496 | 0.494 | 0.486 |
| 6 | 5.5 | 0.341 | 0.271 | 0.262 | 0.145 | 0.190 | 0.169 |
| 7 | 4.5 | 0.463 | 0.412 | 0.309 | 0.307 | 0.353 | 0.224 |
| 9 | 3.5 | | | 0.380 | | | 0.302 |
| 15 | 2.5 | | | 0.478 | | | 0.404 |
| 16 | 6.5 | 0.579 | 0.562 | 0.539 | 0.492 | 0.517 | 0.478 |

[a] Reference 28. [b] State interaction of $^4\Sigma,^4\Pi,^4\Delta,^4\Phi,^4\Gamma,^4$H,$^4$I, $^6$K,$^6\Lambda$. [c] State interaction of $^4\Sigma,^4\Pi,^4\Delta,^4\Phi,^4\Gamma,^4$H,$^4$I, $^4\Phi,\Gamma,^6$H,$^6$I,$^6$K,$^6\Lambda$. [d] SO-CI basis sets: SPP/WB U (14s13p10d8f); AE DKH+BP U (21s18p12d16f); H (7s). [e] SO-CI basis sets: SPP/DC+B U (14s13p10d8f)/[6s6p5d4f]; AE DKH+BP U (30s26p18d14f)/[10s9p7d5f]; H aug-cc-pVQZ. [f] The numbering of the states refers to the energetic ordering at the PP MCDF/DC+B level.

Table 6 lists vertical excitation energies for the ground state internuclear equilibrium distance (2.011 Å). The Ω states were calculated with the state interaction approach, i.e., by diagonalizing a Hamiltonian matrix including the SO terms built in a basis of correlated ΛS states, obtained at the CASSCF/MRCI level. The MAD between the old WB PP and DKH/BP results was 0.078 eV.[28] If the same ΛS states are used to build the SO-CI Hamiltonian matrix ($^4\Sigma,^4\Pi,^4\Delta,^4\Phi,^4\Gamma,^4$H,$^4$I,$^6$K,$^6\Lambda$) this value is decreased to 0.034 eV for the new MCDHF/DC+B PP and the application of generalized contracted basis sets for both the MCDHF/DC+B PP and AE DKH/BP calculations also in the SO-CI. In our present calculations we added four higher ΛS states ($^6\Phi,^6\Gamma,^6$H,$^6$I) and found two additional low-lying Ω states with a term energy below 0.5 eV. The MAD between the MCDHF/DC+B PP and AE DKH/BP results is now 0.041 eV.

**TABLE 7: Contributions (%) of ΛS States to the Ω States for UH at 2.011 Å[a]**

| no. | Ω | ΛS (percentage PP; AE) |
|---|---|---|
| 1 | 4.5 | $^4$I(78; 76) + $^4$H(19; 19) + $^4$Γ(3; 3) + $^6$K(0; 1) |
| 2 | 3.5 | $^4$H(58; 57) + $^4$Γ(31; 30) + $^4$Φ(9; 9) + $^4$Δ(1; 1) + $^6$I(0; 1) + $^6$H(0; 1) |
| 3 | 2.5 | $^4$Γ(42; 41) + $^4$Φ(37; 37) + $^4$Δ(17; 16) + $^4$Π(3; 3) + $^6$Γ(0; 1) + $^6$H(0; 1) |
| 4 | 1.5 | $^4$Δ(40; 39) + $^4$Φ(30; 30) + $^4$Π(24; 24) + $^4$Σ(6; 6) |
| 5 | 0.5 | $^4$Π(49; 49) + $^4$Σ(30; 30) + $^4$Δ(21; 21) |
| 8 | 5.5 | $^4$I(72; 68) + $^4$H(23; 23) + $^4$Γ(3; 3) + $^6$I(0; 2) + $^6$Λ(0; 2) + $^6$K(0; 1) |
| 10 | 4.5 | $^4$H(36; 33) + $^4$Γ(36; 33) + $^4$I(19; 18) + $^4$Φ(9; 8) + $^6$K(1; 3) + $^6$H(0; 2) + $^6$Γ(0; 1) |
| 11 | 3.5 | $^4$Φ(38; 37) + $^4$H(32; 32) + $^4$Δ(16; 16) + $^4$Γ(13; 13) + $^6$Γ(0; 1) |
| 12 | 2.5 | $^4$Γ(38; 41) + $^4$Δ(34; 30) + $^4$Π(23; 21) + $^4$Φ(2; 0) + $^6$H(2; 1) + $^6$Γ(1; 3) + $^6$Φ(0; 1) |
| 13 | 1.5 | $^4$Φ(38; 37) + $^4$Σ(28; 28) + $^4$Π(28; 25) + $^4$Δ(5; 0) + $^6$Γ(1; 7) + $^6$Φ(0; 3) |
| 14 | 0.5 | $^4$Π(41; 43) + $^4$Δ(37; 41) + $^4$Σ(17; 15) + $^4$Φ(4; 0) + $^6$Φ(0; 1) |
| 6 | 5.5 | $^6$Λ(79; 79) + $^6$K(17; 17) + $^4$I(3; 3) |
| 7 | 4.5 | $^6$K(62; 62) + $^6$I(27; 27) + $^6$H(8; 8) + $^6$Γ(2; 2) + $^4$I(1; 2) |
| 9 | 3.5 | $^6$I(49; 49) + $^6$H(34; 33) + $^6$Γ(13; 13) + $^6$Φ(2; 2) + $^4$H(1; 2) |
| 15 | 2.5 | $^4$H(47; 47) + $^6$Γ(38; 36) + $^6$Φ(11; 9) + $^4$Γ(3; 0) + $^4$Δ(0; 4) + $^4$Π(0; 2) + $^4$Φ(0; 1) |
| 16 | 6.5 | $^6$Λ(68; 68) + $^6$K(25; 26) + $^6$I(6; 6) |

[a] For the numbering of states, cf. Table 6. Key: PP, MCDHF/DC+B PP; AE, DKH+BP.

In Table 6 the Ω states are numbered according to increasing energy in the MCDHF/DC+B PP calculations using the largest interacting space: however, they are assigned to three groups according to their ΛS state contributions, which are summarized in Table 7. Unless otherwise noted the following discussion refers to the MCDHF/DC+B PP and AE DKH+BP results obtained with the largest interacting space.

The vertical excitation energies to the lowest excited states (no. 2−5 in Table 6) agree within 0.006 eV for the MCDHF/DC+B PP and DKH/BP results. For the next group of states (no. 8, 10−14) the AE DKH values are by 0.031−0.047 eV higher than the MCDHF/DC+B PP values. The explanation of these small deviations is not straightforward. If one assumes a $U^+$ $H^-$ charge distribution with $U^+$ $5f^3$ $7s^2$ $^4$I and $H^-$ $1s^2$ $^1$S giving rise to the lowest UH states, i.e., Ω = 9/2−1/2 (no. 1−5) from the $U^+$ $^4I_{9/2}$ ground state and Ω = 11/2−1/2 (No. 8, 10−14) from the $U^+$ $^4I_{11/2}$ first excited state, the 0.031−0.047 eV higher AE DKH excitation energies of the second group of states can be partially explained by the fact that the Breit contribution to lower the term energy of the excited $U^+$ $^4I_{11/2}$ state with respect to the $U^+$ $^4I_{9/2}$ ground state by 0.027 eV at the AE MCDHF level.[32] On the other hand the fit of the PP leads to a $U^+$ $^4I_{11/2}$ term energy which is by 0.011 eV too low compared to the AE MCDHF/DC+B reference value. Thus a deviation of about 0.038 eV between the PP MCDHF/DC+B and AE DKH excitation energies for the second group of states (no. 8, 10−14) can be explained by the neglect of the Breit interaction at the DKH level and PP errors.

For the last group of states (no. 6, 7, 9, 15, 16) the MCDHF/DC+B PP values are by 0.06−0.093 eV higher than the AE DKH results. In contrast to the Ω states of first two groups discussed above, for which the leading ΛS contributions stem from quartet states, they arise now from sextet states. Unfortunately we are currently unable to explain the deviations occurring for this group of excited states in a similar manner as above. These states possibly arise from the $U^+$ $5f^3$ $6d^1$ $7s^1$ $^6L_{11/2}$ state, which is experimentally only 289 cm$^{-1}$ above $U^+$ $5f^3$ $7s^2$ $^4I_{9/2}$. However, in this case the sum of PP errors and omission of the Breit interaction amounts to 0.020 eV and thus cannot explain the observed deviations of up to almost 0.1 eV. Most likely these rather arise from differences in the correlation treatment.

At this point we want to mention that recent large scale intermediate Hamiltonian Fock-space coupled-cluster calculations (IH-FSCC)[29,30] for $U^{5+}$ $5f^1$ and $U^{4+}$ $5f^2$ using the PP presented here together with uncontracted basis sets containing up to *i* functions show excellent agreement with corresponding AE calculations using the extrapolated IH-FSCC approach[65] based on the DCB Hamiltonian as well as with experimental data.[31,66] In fact for all levels of $U^{4+}$ $5f^2$ the MAD of the PP results from the AE values is only about 0.02 eV, those from the experimental values about 0.04−0.05 eV depending on the basis set. In view of these atomic results we find the agreement for UH between AE DKH and PP MCDHF/DC+B to be quite satisfactory.

**TABLE 8: Bond Lengths $R_e$ (Å), Vibrational Constants $\omega_e$ (cm$^{-1}$), and Adiabatic Term Energies $T_e$ (eV) of UH from Calculations with Spin−Orbit Coupling (State Interaction Approach)[a]**

| | | $R_e$ | | $\omega_e$ | | $T_e$ | |
|---|---|---|---|---|---|---|---|
| no. | Ω | PP | AE | PP | AE | PP | AE |
| 1 | 4.5 | 2.025 | 2.021 | 1505 | 1511 | 0.000 | 0.000 |
| 2 | 3.5 | 2.026 | 2.021 | 1499 | 1504 | 0.025 | 0.020 |
| 3 | 2.5 | 2.024 | 2.020 | 1496 | 1502 | 0.042 | 0.039 |
| 4 | 1.5 | 2.025 | 2.020 | 1494 | 1502 | 0.054 | 0.053 |
| 5 | 0.5 | 2.027 | 2.021 | 1494 | 1500 | 0.067 | 0.066 |
| 8 | 5.5 | 2.024 | 2.022 | 1505 | 1498 | 0.374 | 0.409 |
| 10 | 4.5 | 2.025 | 2.021 | 1499 | 1497 | 0.401 | 0.432 |
| 11 | 3.5 | 2.023 | 2.019 | 1491 | 1507 | 0.420 | 0.454 |
| 12 | 2.5 | 2.025 | 2.020 | 1479 | 1514 | 0.431 | 0.476 |
| 13 | 1.5 | 2.025 | 2.022 | 1496 | 1481 | 0.448 | 0.476 |
| 14 | 0.5 | 2.024 | 2.019 | 1486 | 1505 | 0.448 | 0.486 |
| 6 | 5.5 | 2.071 | 2.068 | 1428 | 1364 | 0.249 | 0.157 |
| 7 | 4.5 | 2.068 | 2.064 | 1425 | 1372 | 0.296 | 0.211 |
| 9 | 3.5 | 2.067 | 2.063 | 1423 | 1369 | 0.367 | 0.290 |
| 15 | 2.5 | 2.064 | 2.061 | 1451 | 1361 | 0.466 | 0.393 |
| 16 | 6.5 | 2.069 | 2.065 | 1433 | 1370 | 0.527 | 0.467 |

[a] For the numbering of states cf. Table 6. Key: PP, MCDHF/DC+B PP; AE, DKH+BP.

Table 8 finally summarizes the spectroscopic constants of 16 low-lying electronic states of UH. The MAD between MCDHF/DC+B PP and AE DKH+BP bond lengths is only 0.004 Å for all states. For the vibrational constants the corresponding MAD is 28 cm$^{-1}$. This relatively large value results from the significant deviations of the third group of Ω states, which arise manily from sextet states (no. 6, 7, 9, 15, 16). Excluding these Ω states, i.e., taking only those into account which mainly arise from quartet states (no. 1−5, 8, 10−14) leads to a MAD of only 11 cm$^{-1}$. Similarly, the MAD for the adiabatic term energies of all states is 0.040 eV, whereas the one for the Ω states of mainly quartet provenience is only 0.022 eV.

## 4. Conclusion

A new multiconfiguration Dirac−Hartree−Fock adjusted energy-consistent small-core pseudotential for uranium has been presented and was successfully tested in molecular calculations on uranium monohydride. It has been demonstrated that besides the dominating Dirac one-electron relativistic contributions small-core pseudopotentials can also implicitly include contributions such as the Breit interaction and finite nucleus effects with a sufficiently high accuracy. Thus pseudopotentials can model relativistic all-electron approaches which go beyond the Dirac−Coulomb Hamiltonian or approximations thereof, e.g., the Douglas−Kroll−Hess or Chang−Pelissier−Durand Hamiltonians, at a comparatively moderate computational cost.

**Acknowledgment.** This work is dedicated to Professor Russell M. Pitzer on the occasion of his 70th birthday. The development of MCDHF-adjusted pseudopotentials is financially supported by the Deutsche Forschungsgemeinschaft (DFG).

**Supporting Information Available:** Extended version of the Tables 1−3, listings of the pseudopotential and basis set parameters, and scalar-relativistic results for UH. This information is available free of charge via the Internet at http://pubs.acs.org.

## References and Notes

(1) *Relativistic Electronic Structure Theory, Part 1: Fundamentals; Theoretical and Computational Chemistry*; Schwerdtfeger, P., Ed.; Elsevier: Amsterdam, 2002.
(2) *Recent Advances in Relativistic Molecular Theory*; Hirao, K., Ishikawa, Y., Eds.; World Scientific: Singapore, 2004.
(3) Chang, A.; Pitzer, R. M. *J. Am. Chem. Soc.* **1989**, *111*, 2500.
(4) Yabushita, S.; Zhang, Z.; Pitzer, R. M. *J. Phys. Chem. A* **1999**, *103*, 5791.
(5) Vallet, V.; Maron, L.; Teichteil, C.; Flament, J.-P. *J. Chem. Phys.* **2000**, *113*, 1391.
(6) Llusar, R.; Casarrubios, M.; Barandiarán, Z.; Seijo, L. *J. Chem. Phys.* **1996**, *105*, 5321.
(7) Ilias, M.; Kellö, V.; Visscher, L.; Schimmelpfennig, B. *J. Chem. Phys.* **2001**, *115*, 9667.
(8) Dolg, M.; Stoll, H.; Seth, M.; Schwerdtfeger, P. *Chem. Phys. Lett.* **2001**, *345*, 490.
(9) Douglas, M.; Kroll, N. M. *Ann. Phys.* **1974**, *82*, 89.
(10) Hess, B. A. *Phys. Rev. A* **1986**, *33*, 3742.
(11) Jansen, G.; Hess, B. A. *Phys. Rev. A* **1989**, *39*, 6016.
(12) Wolf, A.; Reiher, M.; Hess, B. A. *J. Phys. Chem.* **2002**, *117*, 9215.
(13) Chang, C.; Pélissier, M.; Durand, D. *Phys. Scr.* **1986**, *34*, 394.
(14) Cao, X.; Dolg, M. In *Relativistic Methods for Chemists*; Barysz, M., Ishikawa, Y., Eds.; Springer: Berlin, 2009, in press.
(15) Pepper, M.; Bursten, B. *Chem. Rev.* **1991**, *91*, 719.
(16) Schreckenbach, G.; Hay, P. J.; Martin, R. L. *J. Comput. Chem.* **1999**, *20*, 70.
(17) Dolg, M.; Cao, X. In *Recent Advances in Relativistic Molecular Theory*; Hirao, K., Ishikawa, Y., Eds.; World Scientific: River Edge, NJ, 2004.
(18) Cao, X.; Dolg, M. *Coord. Chem. Rev.* **2006**, *250*, 900.
(19) Lim, I. S.; Schwerdtfeger, P.; Metz, B.; Stoll, H. *J. Chem. Phys.* **2005**, *122*, 104103.
(20) Lim, I. S.; Stoll, H.; Schwerdtfeger, P. *J. Chem. Phys.* **2006**, *124*, 034107.
(21) Metz, B.; Schweizer, M.; Stoll, H.; Dolg, M.; Liu, W. *Theor. Chem. Acc.* **2000**, *104*, 22.
(22) Metz, B.; Stoll, H.; Dolg, M. *J. Chem. Phys.* **2000**, *113*, 2563.
(23) Peterson, K. A.; Figgen, D.; Goll, E.; Stoll, H.; Dolg, M. *J. Chem. Phys.* **2003**, *119*, 11113.
(24) Figgen, D.; Rauhut, G.; Dolg, M.; Stoll, H. *Chem. Phys.* **2005**, *311*, 227.
(25) Dolg, M. *Theor. Chem. Acc.* **2005**, *114*, 297.
(26) Peterson, K. A.; Figgen, D.; Dolg, M.; Stoll, H. *J. Chem. Phys.* **2007**, *126*, 124101.
(27) Figgen, D.; Peterson, K. A.; Dolg, M.; Stoll, H. *J. Chem. Phys.* **2009**, *130*, 164108.
(28) Cao, X.; Moritz, A.; Dolg, M. *Chem. Phys.* **2008**, *343*, 250.
(29) Eliav, E.; Kaldor, U.; Ishikawa, Y. *Phys. Rev. A* **1994**, *49*, 1724.
(30) Landau, A.; Eliav, E.; Ishikawa, Y.; Kaldor, U. *J. Chem. Phys.* **2001**, *115*, 6862.
(31) Weigand, A.; Cao, X.; Vallet, V.; Flament, J.-P.; Dolg, M. *J. Phys. Chem A* 2009. submitted (W. Thiel Festschrift).
(32) Dyall, K. G.; Grant, I. P.; Johnson, C. T.; Parpia, F. A.; Plummer, E. P. *Comput. Phys. Commun.* **1989**, *55*, 425. atomic structure code GRASP; extension for pseudopotentials by M. Dolg and B. Metz. .
(33) Amos, R. D.; Bernhardsson, A.; Berning, A.; Celani, P.; Cooper, D. L.; Deegan, M.; J, O.; Dobbyn, A. J.; Eckert, F.; Hampel, C.; Hetzer, G.; Knowles, P. J.; Korona, T.; Lindh, R.; Lloyd, A. W.; McNicholas, S. J.; Manby, F. R.; Meyer, W.; Mura, M. E.; Nicklass, A.; Palmieri, P.; Pitzer, R.; Rauhut, G.; Schütz, M.; Schuhmann, U.; Stoll, H.; Tarroni, A. J. S. R.; Thorsteinsson, T.; Werner, H. J. *MOLPRO is a Package of ab Initio Programs*; University of Birmingham, 2002.
(34) Dunning, T. H. *J. Chem. Phys.* **1989**, *90*, 1007.
(35) Christiansen, P. A.; Lee, Y. S.; Pitzer, K. S. *J. Chem. Phys.* **1979**, *71*, 4445.
(36) Ermler, W. C.; Ross, R. B.; Christiansen, P. A. *Adv. Quantum Chem.* **1988**, *19*, 139.
(37) Wood, J. H.; Boring, A. M. *Phys. Rev. B* **1978**, *18*, 2701.
(38) Cowan, R. D.; Griffin, D. C. *J. Opt. Soc. Am.* **1976**, *66*, 1010.
(39) Hay, P. J.; Wadt, W. R. *J. Chem. Phys.* **1985**, *82*, 270.
(40) Hay, P. J.; Wadt, W. R. *J. Chem. Phys.* **1985**, *82*, 299.
(41) Wadt, W. R.; Hay, P. J. *J. Chem. Phys.* **1985**, *82*, 284.
(42) Dolg, M. In *Modern Methods and Algorithms of Quantum Chemistry*; Grotendorst, J., Ed.; NIC Series, 2000; Vol. 1, pp 479−508; Vol. 3, pp 507−540.
(43) Stoll, H.; Metz, B.; Dolg, M. *J. Comput. Chem.* **2002**, *23*, 767.
(44) Seijo, L.; Barandiarán, Z. In *Computional chemistry: Reviews of current trends*; Leszczynski, J., Ed.; World Scientific: Singapore, 1999; Vol. 4, pp 55−152.
(45) Mosyagin, N. S.; Petrov, A. N.; Titov, A. V.; Tupitsyn, I. I. *Recent Advances in the Theory of Chemical and Physical Systems*; Julien, J. P., Maruani, J., Mayou, D., Eds.; Progress in Theoretical Chemistry and Physics, Part II, Springer: Berlin, 2006; Vol. 15, pp 253−284.
(46) Moritz, A.; Cao, X.; Dolg, M. *Theor. Chem. Acc.* **2007**, *117*, 473.
(47) Moritz, A.; Cao, X.; Dolg, M. *Theor. Chem. Acc.* **2007**, *118*, 2763.
(48) Moritz, A.; Dolg, M. *Theor. Chem. Acc.* **2008**, *121*, 297.
(49) Field, R. W. *Ber. Bunsen-Ges. Phys. Chem.* **1982**, *86*, 771.
(50) Cao, X.; Li, Q.; Moritz, A.; Xie, Z.; Dolg, M.; Chen, X.; Fang, W. *Inorg. Chem.* **2006**, *45*, 3444.
(51) Wiebke, J.; Moritz, A.; Cao, X.; Dolg, M. *Phys. Chem. Chem. Phys.* **2007**, *9*, 459.
(52) Moritz, A.; Dolg, M. *Chem. Phys.* **2007**, *327*, 48.
(53) Küchle, W.; Dolg, M.; Stoll, H.; Preuss, H. *J. Chem. Phys.* **1994**, *100*, 7535.
(54) Cao, X.; Dolg, M.; Stoll, H. *J. Chem. Phys.* **2003**, *118*, 487.
(55) Dolg, M.; Stoll, H.; Preu$\beta$, H. *J. Chem. Phys.* **1989**, *90*, 1730.
(56) Cao, X.; Dolg, M. *J. Chem. Phys.* **2001**, *115*, 7348.
(57) Dolg, M. *J. Chem. Phys.* **1996**, *104*, 4061.
(58) Dolg, M. *Chem. Phys. Lett.* **1996**, *250*, 75.
(59) Pittel, B.; Schwarz, W. H. E. *Chem. Phys. Lett.* **1977**, *46*, 121.
(60) Teichteil, C.; Malrieu, J. P.; Barthelat, J. C. *Mol. Phys.* **1977**, *33*, 181.
(61) Pitzer, R. M. *Atomic Electronic Structure Code ATMSCF*; The Ohio State University: Columbus, OH, 1979.
(62) Souter, P. F.; Kushto, G. P.; Andrews, L.; Neurock, M. *J. Am. Chem. Soc.* **1997**, *119*, 1682.
(63) Balasubramanian, K.; Siekhaus, W. J.; McLean, W., II *J. Chem. Phys.* **2003**, *119*, 5889.
(64) Raab, J.; Lindh, R. H.; Wang, X.; Andrews, L.; Gagliardi, L. *J. Phys. Chem. A* **2007**, *111*, 6383.
(65) Eliav, E.; Vilkas, M. J.; Ishikawa, Y.; Kaldor, U. *J. Chem. Phys.* **2005**, *122*, 224113.
(66) Infante, I.; Eliav, E.; Vilkas, M. J.; Ishikawa, Y.; Kaldor, U.; Visscher, L. *J. Chem. Phys.* **2007**, *127*, 124308.

JP9044594